Central European Journal of Energetic Materials
ISSN 1733-7178; e-ISSN 2353-1843

Cent. Eur. J. Energ. Mater. 2019, *16*(1): 21-32; DOI: 10.22211/cejem/104390
Article is available in PDF-format, in colour, at: http://www.wydawnictwa.ipo.waw.pl/CEJEM.html

Research paper

Shock Ignition and Growth of HMX-based PBXs under Different Temperature Conditions

Rui Liu, Yong Han,* Ming Li, Zhihai Jiang, Songwei He

Institute of Chemical Materials, China Academy of Engineering Physics, 64 Mianshan Road, Mianyang, Sichuan 621900, China
**E-mail: y_han76@126.com*

Abstract: The Lagrange test was conducted to investigate the shock ignition and growth of HMX-based polymer bonded explosives (PBXs) under different temperature conditions. In this study, three temperature conditions, 25 °C, 80 °C and 120 °C were used. The pressure history values along the direction of the detonation wave propagation were obtained and presented as the characteristics of the shock ignition and growth. Manganin piezoresistive pressure gauges were used to measure the pressure. The results showed that the distance to detonation was clearly reduced as the temperature was increased. A distance greater than 9 mm at 25 °C was changed to less than 3 mm at 120 °C. In order to understand this phenomenon in more detail, the Lee-Tarver ignition and growth model was employed to simulate the Lagrange test, and the simulated pressures were compared with the measured pressures. The results demonstrated that the intrinsic mechanism of the phenomenon was that the high temperature changed both the equation of state of the unreacted explosive and the chemical reaction rate. It was remarkable that the parameter R_2 in the model was reduced from −0.05835 to −0.06338, and the parameter G_1 in the model was increased from 1.3 to 2.12.

Keywords: shock ignition and growth, Lagrange test, HMX-based PBXs, high temperatures, Lee-Tarver model

1 Introduction

The shock ignition and growth phenomenon of polymer bonded explosives (PBXs) has been a research focus for several decades [1]. The mechanism of the phenomenon is related to the chemical reaction rate of the explosive. Therefore, it is meaningful to understand the relationship between the chemical reaction and shock ignition and growth.

The Lagrange analysis method, as an experimental method, was developed to analyze the flow field after the shock wave. This included the particle velocity and pressure measurements. Particle velocity measurement was mainly based on electromagnetic technology. Stennett *et al.* [2] used electromagnetic particle velocity gauges to record the onset of reaction of a PBX under impact. Gustavsen *et al.* [3] designed a 12-channel dense particle velocity wave profile measurement in a single experiment for the shock initiation behaviour of PBX9501. The results showed that the shock initiation was sensitive to the density, but insensitive to the ageing conditions [3]. For pressure measurements, the *in-situ* manganin piezoresistive pressure gauge has been widely used. Chidester *et al.* [4] obtained pressure gauge data for PBX9501 under impact, where the input pressure was below 3 GPa. Hussain *et al.* [5] analyzed the particle size effect on the shock ignition and growth of PBXs by means of pressure profiles.

The environmental temperature has been demonstrated to influence shock ignition and growth of PBXs [6-8]. Tarver *et al.* [9] conducted a series of experiments on the HMX-based explosive PBX9501 at initial temperatures 25 °C and 50 °C under plate impact. Measured run distances to detonation were obtained. Tan *et al.* [10] also discussed the shock initiation characteristics of HMX/TATB composite explosives at near-ambient temperatures, from 5 °C to 75 °C. The results showed that the effects of the near-ambient temperature could not be ignored. Urtiew *et al.* [11] investigated HMX-based explosives at 170 °C under fragment impact. The shock sensitivity of HMX at 170 °C was greater than that at ambient temperature. Note that there is a phase transformation of HMX above 165 °C.

In order to understand the mechanism of shock ignition and growth of PBXs, several classical models have been developed. The Lee-Tarver ignition and growth model has been widely applied in this field [12, 13]. The early Lee-Tarver ignition and growth model only considered hotspot formation and growth of the reaction. In a subsequent development, a completion growth term was added in the Lee-Tarver ignition and growth model, in order to successfully simulate the response under high pressure and short duration shocks [14]. May and Tarver [15] applied the model to simulate the shock ignition under flyer plate impacts. Garcia *et al.* [16] applied the Lee-Tarver ignition model to simulate the shock initiation of low density HMX and obtained good agreement with the experimental results. In addition, the model has also been employed to describe the shock ignition of PBXs at different temperatures [9-11]. Generally, the Lee-Tarver ignition model has good capability to simulate the shock ignition of PBXs under complex conditions, while the calculated results can successfully match experiments.

In the present study, the shock ignition and growth of HMX-based explosives under high temperature conditions was studied. Three different temperature conditions, 25 °C, 80 °C and 120 °C were used. The temperature conditions were below that of the phase transformation of HMX. A heating arrangement was applied to control the temperature. As described above, Lagrange shock ignition tests were conducted, and manganin piezoresistive pressure gauges were applied to measure the pressure. Furthermore, the Lee-Tarver ignition model was used to explain the mechanism of the ignition and growth on exposure to the temperature.

2 Experimental

In order to understand the shock ignition and growth of HMX-based PBXs under different temperature conditions, the classical Lagrangian test was conducted. Figure 1 shows a schematic diagram of the experimental arrangement. A detonator excited a primary explosive, which supplied a high pressure, above 30 GPa. It should be mentioned that the dimensions of the primary explosive were ϕ 50 mm × 50 mm, and the primary explosive was in a stable detonation. Furthermore, the output pressure of the primary explosive was reproducible. A 35 mm thick aluminum plate was arranged between the primary explosive and the explosive specimen under test. Due to the plate, the high pressure was reduced to an appropriate pressure input. In order to observe the phenomenon of the shock ignition and growth of the PBXs, a low pressure input was reasonable. Otherwise, a high pressure input would probably force the ignition to detonation in a very short time. A preliminary test was applied to determine the appropriate thickness of the aluminum plate (35 mm), and the pressure after attenuation could be much lower than 30 GPa. The specimens consisted of four ϕ 50 mm × 3 mm discs, and a group of manganin piezoresistive gauges were arranged at the top of each disk, corresponding to distances of 0 mm, 3 mm, 6 mm and 9 mm, respectively, which is presented in the side view of the experimental arrangement (see Figure 1). It should be stressed that a thin Teflon® insulation sheet encapsulated the gauges, in order to avoid short circuit of the gauges due to the explosion. In using the gauges, a high-speed constant-current synchronised source was used to supply the power, with an oscilloscope to record the voltage temporal curve, which could then be converted to a pressure history curve. In our study, three different temperatures, 25 °C, 80 °C and 120 °C, were used. A heating system was designed to control the temperature of the specimens. Temperature control tests were performed before the Lagrangian tests, in order to ensure that the temperature of the specimen at each point was uniform. The results showed that the specimens had to be heated for at least 50 min and 120 min to reach 80 °C and 120 °C, respectively.

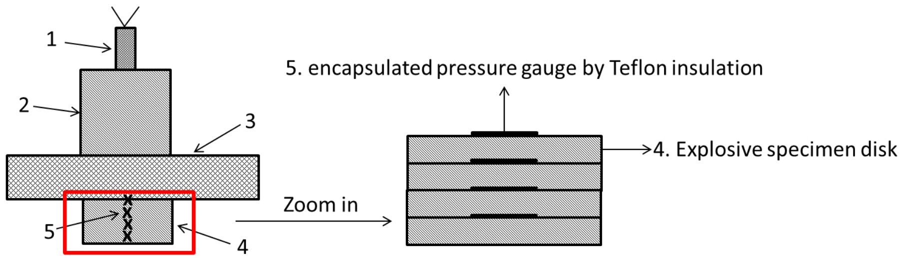

Figure 1. A schematic diagram of the shock ignition and growth arrangement for HMX-based PBXs at different temperatures: 1) detonator; 2) primary explosive; 3) aluminum plate; 4) explosive specimen disk; 5) encapsulated pressure gauge with Teflon® insulation

3 Ignition and Growth Modelling

Ignition and growth modelling of PBXs based on the Lee-Tarver phenomenological model [12] was applied to understand the response of the specimens at different temperatures. The model was as shown in Equation 1:

$$\frac{d\lambda}{dt} = I(1-\lambda)^b\left(\frac{\rho}{\rho_0} - 1 - a\right)^x + G_1(1-\lambda)^c\lambda^d P^y + G_2(1-\lambda)^e\lambda^g P^z \tag{1}$$

where λ is the chemical reaction degree, t is the time, ρ is the density of the specimen, ρ_0 is the initial density of the specimen, P is the pressure, and other parameters, I, G_1, G_2, a, b, x, c, d, y, e, g and z, are constants.

The Lee-Tarver model has a good physical meaning for explaining the shock ignition phenomenon. The first term of Equation 1 represents the ignition of the specimen due to shock compression. The parameters in the first term control the quantity of hot spots. The second term of Equation 1 represents a slow reaction to produce gas. The parameters in the second term control the initial reaction based on the hot spots. The third term of Equation 1 represents a rapid completion of the reaction at high pressure and temperature.

For ignition and growth modelling, the equation of state of the unreacted explosives and the reaction products is required. A Jones-Wilkins-Lee (JWL) equation of state is always applied for the unreacted explosives and the reaction products as Equations 2 and 3, respectively [17-19]:

$$P_e = R_1 e^{-R_5 V_e} + R_2 e^{-R_6 V_e} + R_3 \frac{T_0}{V_e} \quad (R_3 = \omega_e C_{\mathrm{ve}}) \tag{2}$$

$$P_p = A e^{-x_{p1} V_p} + B e^{-x_{p2} V_p} + g_1 \frac{T_p}{V_p} \quad (g_1 = \omega_p C_{\mathrm{vp}}) \tag{3}$$

where P is the pressure, the parameters R_1, R_2, R_3, R_5, R_6, A, B, x_{p1}, x_{p2}, g_1, ω are constants, C_v is the heat capacity, T_0 is the initial temperature of the specimen and T_p is the temperature of the products. Note that the subscripts e and p represent the unreacted explosive and the reaction products, respectively. The parameters at the temperature of 25 °C are listed in Table 1 [20].

Table 1. Parameters for the ignition and growth modelling (temperature = 25 °C)

I	a	b	c	x	G_1
6.43×10^{11}	0.16	0.667	0.667	20	1.3
d	y	G_2	e	g	z
0.111	1	400	0.333	0.579	2.1705
R_1	R_2	R_3	R_5	R_6	
9722	−0.05835	2.4656×10^{-5}	14.1	1.41	
A	B	x_{p1}	x_{p2}	g_1	
8.524	0.1802	4.55	1.3	3.8×10^{-4}	

For the primary explosive, the high explosive burn model and the JWL equation of state of the gaseous products were applied to describe the detonation phenomenon. The simulation pressure was close to the detonation pressure of the primary explosive. It should be mentioned that the JWL equation of state was also presented as Equation 3. Considering that the primary explosive was HMX-based, the parameters of the JWL equation of gaseous products for the primary explosive were consistent with those parameters A, B, x_{p1}, x_{p2}, g_1 in Table 1.

The metal plate was applied to control the input pressure acting on the specimen by means of its thickness. In this study, aluminum was employed. Generally the Gruneisen equation of state could describe the mechanical behaviour of aluminum under shock conditions. The parameters are listed in Table 2.

Table 2. Gruneisen parameters for the aluminum plate

ρ [kg·m^{-3}]	C [m·s^{-1}]	s_1	s_2	s_3	γ_0	a
2770	5330	1.338	0	0	2.13	0.666

The commercial software Ls-dyna was used for this simulation. The materials' models and parameters have been explained above. Additionally, considering the structure of the experimental arrangement was axially symmetric, only a 2D computation model was built in order to avoid time consuming computation.

4 Results and Discussion

Figure 2 shows the pressure measurements at different positions, 0 mm, 3 mm, 6 mm and 9 mm, respectively, based on the pressure gauges under the different temperature conditions. The pressure gauges successfully measured the characteristics of the pressure during ignition and growth of the specimen. The pressure obviously grew along the propagation wave, and displayed the typical shock to detonation phenomenon. For the three temperature conditions, the input pressure was consistent due to pressure control by means of the aluminum plate. The growth of the input pressure was visible, while the rise time duration of the pressure at each distance became shorter as the ambient temperature was increased. Notice that at the positions 3 mm, 6 mm and 9 mm, after the pressure peak, the explosive products expanded and followed the entropy principle. Furthermore, the pressure decreased.

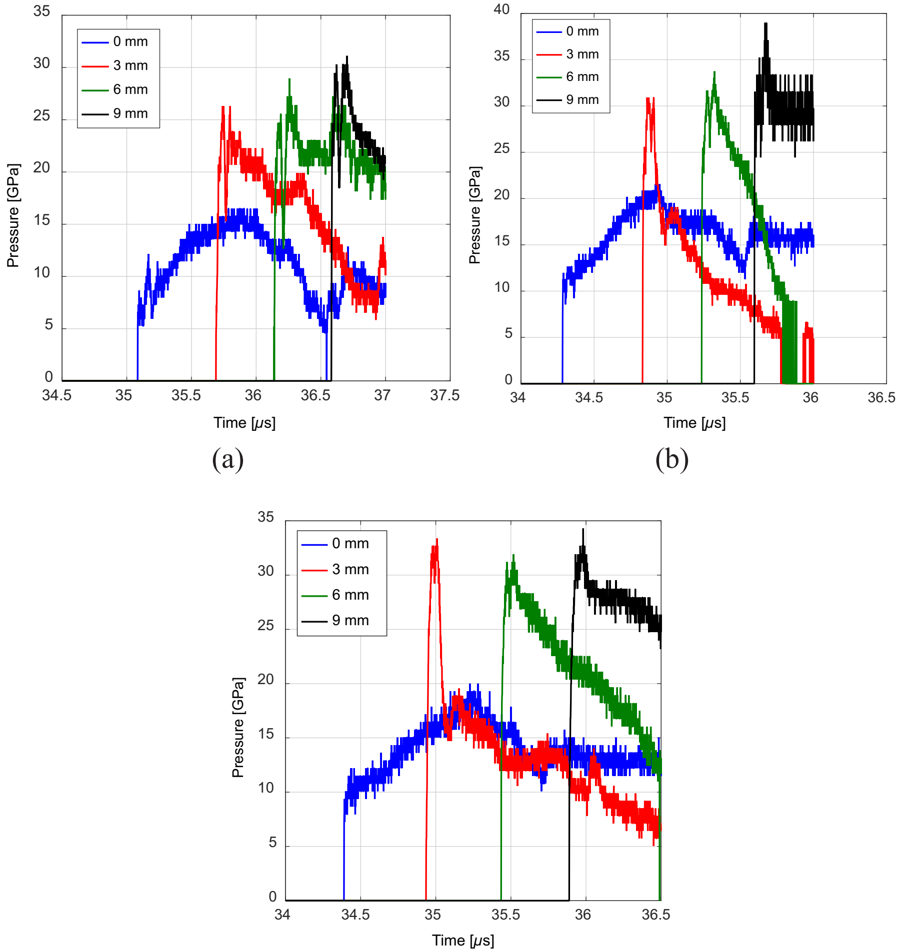

(a) (b) (c)

Figure 2. Pressure history under different temperature conditions based on the pressure gauges: (a) 25 °C; (b) 80 °C; (c) 120 °C

The peak pressures at different positions were noted. For the different temperature conditions, the trends of the peak pressures at different positions are presented in Figure 3. For the three conditions, the input pressure was around 10 GPa. Due to the reaction, the peak pressure at the input position increased to around 16.5 GPa, 21.4 GPa and 19.3 GPa for temperatures 25 °C, 80 °C and 120 °C, respectively. Meanwhile, at positions 3 mm and 6 mm, in the case of temperature 25 °C, the peak pressure exhibited a growth trend, but was less than 30 GPa. By contrast, in the cases of the higher temperatures

80 °C and 120 °C, the peak pressure was higher than 30 GPa. At position 9 mm, in the case of the low temperature experiment, the peak pressure was slightly higher than 30 GPa, while at the high temperatures, the peak pressure was around 35 GPa, which was the detonation pressure of the specimen under study. In the case of 120 °C, at position 6 mm the pressure was reduced slightly, while at position 9 mm the pressure was increased slightly. A similar interesting phenomenon was also observed by Tan [10]. This was probably because the equation of state of the unreacted explosives was changed. As the temperature was increased, the specimen has an obvious volume expansion. In addition, the distance of the shock to detonation transient was not less than 9 mm, between 3 mm and 6 mm, and less than 3 mm, with respect to the three temperatures respectively. In order to determine the distance accurately, a complete pressure history measurement for smaller measured distances would be required.

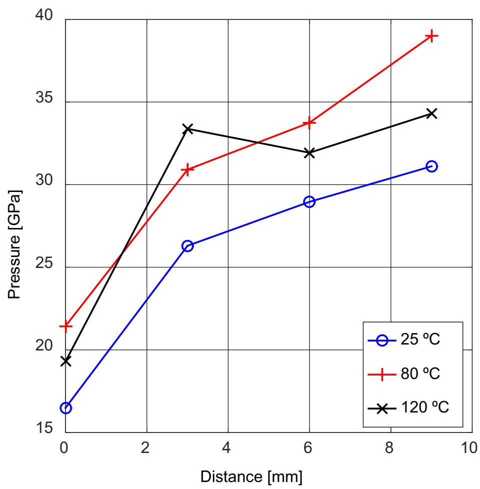

Figure 3. The trend of the peak pressures at different positions under different temperature conditions

The simulations were conducted based on the Lee-Tarver ignition and growth model. Figure 4 shows a comparison between the simulation and the experimental results under the different temperature conditions. Although there was a slight discrepancy in the shock arrival time, the Lee-Tarver ignition and growth model was able to describe the main pressure characteristics.

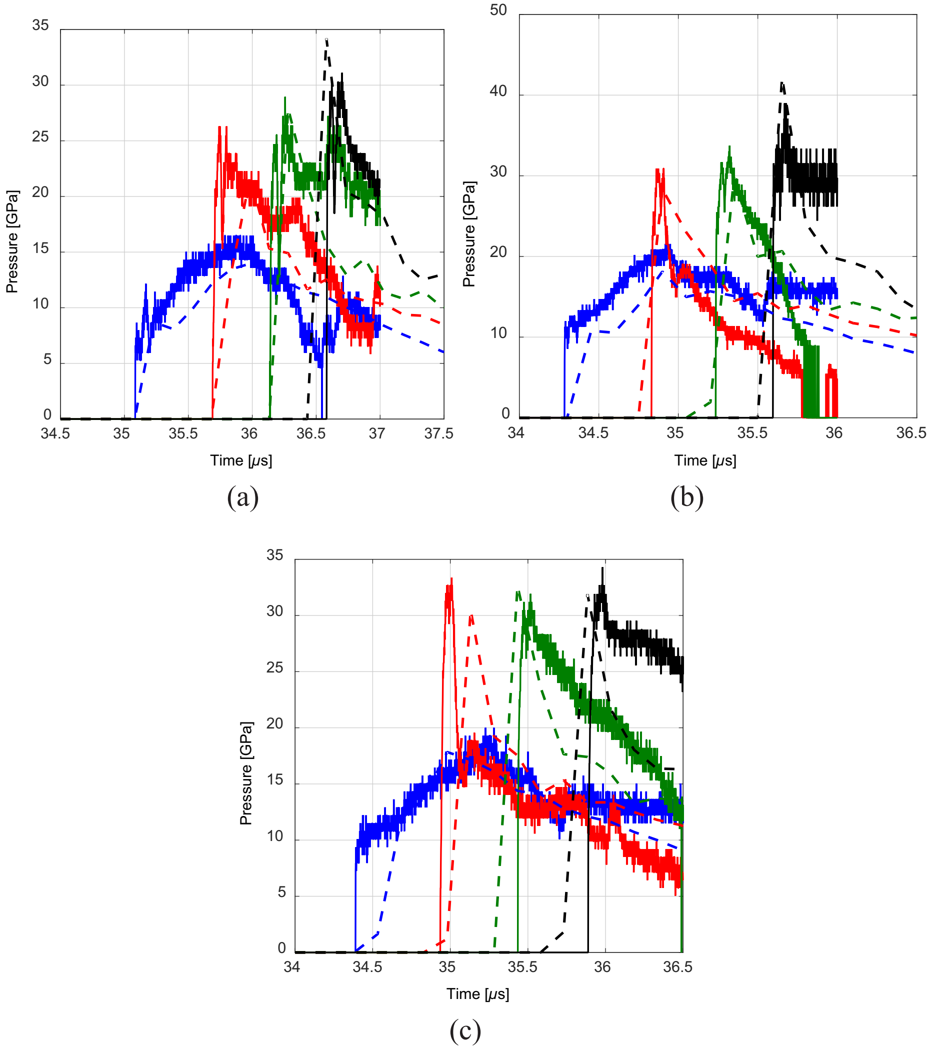

Figure 4. Comparison between the experimental (solid lines) and the simulation (dashed lines) results for distances 0 mm (blue), 3 mm (red), 6 mm (green) and 9 mm (black), under different temperature conditions: (a) 25 °C; (b) 80 °C; (c) 120 °C

In order to match the experimental and the simulation results, two critical parameters, R_2 in the equation of state of the unreacted explosive (see Equation 2) and G_1 in the chemical reaction rate (see Equation 3), were adjusted. Figure 5 shows the trends of these two parameters R_2 and G_1 under the different temperature conditions. When the temperature was increased from 25 °C to 120 °C, the parameter R_2 was reduced by ~8%, from –0.05835 to –0.06338. The parameter G_1 was increased by ~60%, from 1.3 to 2.12. Due to the high temperature, on the one hand, the mechanical behaviour of the unreacted explosive was changed. The materials could be compressed more easily due to thermal softening at high temperature. This resulted in the change in parameter R_2. On the other hand, the temperature conditions could influence the chemical reaction rate. At the high temperature, the energetic materials became more active, and the burning process especially would be accelerated, which is related to parameter G_1. As the experimental results showed, a higher temperature resulted in faster chemical reaction and the shock wave could be quickly increased up to the detonation. In addition, considering that the temperature 120 °C is well below the phase transformation of HMX, the intrinsic mechanism of the change of the ignition and growth could be confirmed as due to the equation of state of the unreacted explosive and the chemical reaction rate.

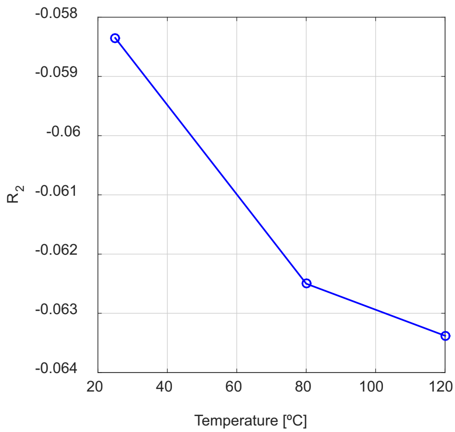

(a)

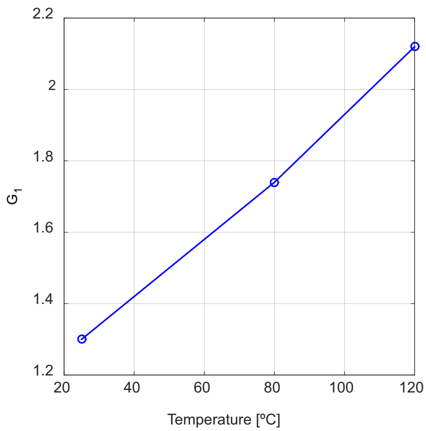

(b)

Figure 5. The trend of parameter R_2 (a) and G_1 (b) under different temperature conditions

5 Conclusions

The shock ignition and growth of HMX-based PBXs under different temperatures conditions was studied. The temperature range was from 25 °C to 120 °C, which is probably encountered during the application of PBXs. The Lagrange experiments based on the pressure gauge technique were successfully conducted. The pressure history showed that the distance of the shock to detonation transition was clearly reduced as the temperature was increased. When the temperature was 25 °C, the distance was not less than 9 mm. In case of 80 °C, the distance was between 3 mm to 6 mm, and when the temperature was 120 °C, the distance was less than 3 mm. The Lee-Tarver ignition and growth model was applied to simulate the experiments. This demonstrated that the model could adequately describe the phenomenon. Due to the temperature range without phase transformations, the change in temperature would influence the equation of state of the unreacted explosive and the chemical reaction rate. The high temperature resulted in a reduction of the parameter R_2 by ~8% and an increase of the parameter G_1 by ~60%.

References

[1] Horie, Y. *Shock Wave Science and Technology Reference Library Volume 3, Solids II*, Springer, **2009**, pp. 1-59; ISBN 978-3-540-77078-7.

[2] Stennett, C.; Cooper, G. A.; Hazell, P. J.; Appleby-Thomas, G. Initiation of Secondary Explosives Measured Using Embedded Electromagnetic Gauges. *Proc. APS-GSCCM*, Melville, U.S.A., **2009**, 267-270.

[3] Gustavsen, R. L.; Sheffield, S. A.; Alcon, R. R.; Hill, L. G. *Shock Initiation of New and Aged PBX9501 Measured with Embedded Electromagnetic Particle Velocity Gauges.* Los Alamos Report LA-13634-MS, **1999**.

[4] Chidester, S. K.; Thompson, D. G.; Vandersall, K. S.; Idar, D. J.; Tarver, C. M.; Garcia, F.; Urtiew, P. A. Shock Initiation Experiments on PBX9501 Explosive at Pressures Below 3 GPa with Associated Ignition and Growth Modeling. *AIP. Conf. Proc.* **2007**, *955*: 903-906.

[5] Hussain, T.; Liu, Y.; Huang, F. L.; Duan, Z. P. Ignition and Growth Modeling of Shock Initiation of Different Particle Size Formulations of PBXC03 Explosive. *J. Energ. Mater.* **2016**, *34*: 38-48.

[6] Duan, Z. P.; Liu, Y. R.; Zhang, Z. Y.; Ou, Z. C.; Huang, F. L. Prediction of Initial Temperature Effects on Shock Initiation of Solid Explosives by Using Mesoscopic Reaction Rate Model. *Int. J. Nonlin. Sci. Num.* **2014**, *15*: 299-305.

[7] Forbes, J. W.; Tarver, C. M.; Urtiew, P. A.; Garcia, F. The Effects of Confinement and Temperature on the Shock Sensitivity of Solid Explosives. *11th Int. Det. Symp.,* Snowmass, USA, **1998**.

[8] Shaw, M. S.; Menikoff, R. A Reactive Burn Model for Shock Initiation in a PBX: Scaling and Separability Based on the Hot Spot Concept. *14th Int. Det. Symp.*, Coeur d'Alene, Idaho, USA, **2010**.

[9] Tarver, C. M.; Forbes, J. W.; Garcia, F.; Urtiew, P. A. Manganin Gauge and Reactive Flow Modeling Study of the Shock Initiation of PBX9501. *AIP. Conf. Proc.***2002**, *620*: 1043-1046.

[10] Tan, K. Y.; Wen, S. G.; Han, Y. Shock Initiation Characteristics of Explosives at Near-ambient Temperatures. *Chin. J. Energ. Mater.* **2016**, *24*: 905-910.
[11] Urtiew, P. A.; Tarver, C. M.; Forbes, J. W.; Garcia, F. Shock Sensitivity of LX-04 at Elevated Temperatures. *AIP Conf. Proc.* **1997**, *429*: 727-730.
[12] Lee, E. L.; Tarver, C. M. Phenomenological Model of Shock Initiation in Heterogeneous Explosives. *Phys. Fluids* **1980**, *23*: 2362-2372.
[13] Tarver, C. M.; Hallquist, J. O.; Erickson, L. M. Modelling Two-dimensional Shock Initiation and Detonation Wave Phenomena in PBX-9404 and LX-17. *7th Int. Det. Sym.*, Annaplis, USA, **1981**.
[14] Whitworth, N. *Mathematical and Numerical Modeling of Shock Initiation in Heterogeneous Solid Explosives*. Cranfield University, Doctoral Dissertation, **2008**.
[15] May, C. M.; Tarver, C. M. Modeling Short Shock Pulse Duration Initiation of LX-16 and LX-10 Charges. *AIP Conf. Proc.* **2010**, *1195*: 275-278.
[16] Garcia, F.; Vandersall, K. S.; Tarver, C. M. Shock Initiation Experiments with Ignition and Growth Modeling on Low Density HMX. *J. Phys. Conf. Ser.* **2014**, *500*: 052048.
[17] Baudin, G.; Serradeill, R. Review of Jones-Wilkins-Lee Equation of State. *EPJ Web Conf.* **2010**, *10*: 00021.
[18] Price, M. A.; Ghee, A. H. Modeling for Detonation and Energy Release from Peroxides and Non-ideal Improvised Explosives. *Cent. Eur. J. Energ, Mater.* **2009**, *6*: 239-254.
[19] Sutton, B. D.; Ferguson, J. W.; Hodgson, A. N. An Analytical Approach to Obtaining JWL Parameters from Cylinder Tests. *AIP Conf. Proc.* **2017**, *1793*: 030032.
[20] Sun, C. W.; Wei, Y. Z.; Zhou, Z. K. *Applied Detonation Physics.* Chinese National Defense Industry Press, **2000**, pp. 337-384; ISBN 7-118-02336-1/O-152.

Received: June 25, 2018
Revised: November 15, 2018
First published online: March 5, 2019